EXPERIMENTAL AND THEORETICAL STUDY ON CATION RADICALS
OF CYCLOPROPANE, CYCLOBUTANE AND CYCLOPENTANE

K. OHTA *, H. NAKATSUJI

Department of Hydrocarbon Chemistry, Faculty of Engineering, Kyoto University, Kyoto, Japan

and

H. KUBODERA and T. SHIDA

Department of Chemistry, Faculty of Science, Kyoto University, Kyoto, Japan

Cation radicals of cycloalkanes have been produced for the first time in γ-irradiated rigid solutions using fluoromethane as a matrix. Observed ESR spectra are analyzed by ab initio MO calculations; molecular geometries of the cations are optimized for several low-lying doublet states by the energy gradient method. Based on the optimized geometry thus determined the hyperfine splitting constants are calculated by the pseudo-orbital theory. Large Jahn–Teller distortions are calculated for the carbon rings and the H–C–H frames of the cation radicals. The distortions are consistent with the nodal picture of singly occupied orbitals. The calculated hfs constants are sensitive to the change in geometry due to a large contribution of spin-delocalization. The average of the calculated proton hfs constants is compatible with the observed ESR spectra which indicates that all the protons of the individual cations have become equivalent owing to the dynamic Jahn–Teller distortion.

1. Introduction

During the past two decades the Jahn–Teller effect in orbitally degenerate polyatomic radicals has been extensively studied both theoretically and experimentally [1]. Among the theoretical studies is the work of Borden, Davidson and co-workers on the geometries of π-radicals [2]. Experimental studies on the ESR lineshape of aromatic hydrocarbon ions and radicals [3] as well as the vibrational analysis of photoelectron spectra of symmetric molecules [4] are numerous.

However, ESR studies of σ-cations of symmetric molecules have been reported only recently [5,6]. In this paper we extend our preliminary study on the cation radicals of cycloalkanes [5] focusing on the comparison between experiment and ab initio MO cal-

culations for the molecular geometry and the spin density distribution. The application of the popular semiempirical INDO method based on a rough guess of the molecular geometry fails because the non-rigid ring motion of the cycloalkane cations affects sensitively the spin density distribution of the non-planar cations. Since the removal of a σ-bonding electron from its parent molecule may result in a significant change in molecular geometry and spin density, a rather detailed study of the geometry should be a prerequisite. As a result of the calculation of the molecular geometry, the cation radicals of cyclopropane and cyclobutane in the ground electronic state are predicted to be distorted from D_{3h} to C_{2v} and from D_{2d} to D_2, respectively, in accordance with the JT theorem. The distortion in the cation radial of cyclopentane from D_{5h} is found to be greater than the distortion in the neutral molecule which is well known to undergo pseudo-rotation between the C_s and C_2 conformations [7].

---

* Present address: Institute for Molecular Science, Myodaiji, Okazaki 444, Japan.

Based on the molecular geometries determined, the hyperfine splitting (hfs) constants are calculated by the pseudo-orbital (PO) theory [8–10] and compared with observed ESR spectra of the cation radicals. It is inferred that the cation radical of cyclopropane undergoes facile dynamic JT distortions at 77 K whereas the cation radical of cyclopentane is subject to the dynamic JT effect at $\approx$100 K because the observed hfs constants at these temperatures are in agreement with the average of the calculated hfs constants.

2. Experimental

Recently it has been established that γ-irradiation of frozen solutions in a CCl_3F matrix leads to an efficient production of cation radicals of solute molecules and their ESR spectra can be measured without significant interference from paramagnetic species produced concomitantly [6,11–14]. We applied this method to obtain ESR spectra of cation radicals of cyclopropane and cyclopentane [‡]. Experimental procedures for irradiation and ESR measurements have been described [11]. Cyclopropane and cyclopentane were commercially obtained and used as received. The ESR measurements were carried out between 77 and $\approx$140 K by using a JEOL FE spectrometer.

3. Experimental results

Fig. 1 illustrates observed ESR spectra of γ-irradiated solutions of cyclopropane in CCl_3F (1 mol) at 77 K (fig. 1a) and cyclopentane in CCl_3F (1 mol) at 77 K and at 100 K (figs. 1b and 1c). The g-values of these cations were determined as $g = 2.0035 \pm 0.0005$ for cyclopropane and 2.0029 ± 0.0005 for cyclopentane. These values are within the range of typical hydrocarbon radicals [12,15]. The spectrum in fig. 1a did not change appreciably upon warming to 100 K whereas the marked spectral change between figs. 1b and 1c was reversible. Upon further warming towards
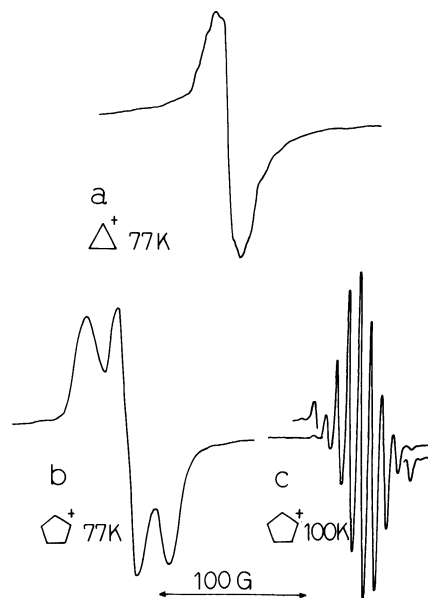
[‡] A preliminary report was present at the 23rd Symposium of Radiation Chemistry, Kyoto, October 1980. We are currently studying cyclobutane which was a kind gift from Professor H. Schwarz of the Institute of Organic Chemistry, Technische Hochschule, Berlin.

Fig. 1. Observed ESR spectra of cation radicals of cycloalkanes in CCl_3F at 77 K. (a) Cyclopropane at 77 K, (b) and (c) cyclopentane at 77 and 100 K. Spectra in (b) and (c) change reversibly.

the melting point of CCl_3F (162 K) part of the spectra changed irreversibly indicating subsequent chemical reactions which we are not interested in at the moment.

By analogy with the results for a number of aliphatic hydrocarbons in CCl_3F [6,11–14] the spectra in fig. 1 are assigned to the cation radicals of the respective cycloalkanes. This is the first example of σ-cations of cycloalkanes. The reversible appearance of the eleven-line spectrum on warming the cyclopentane solution strongly suggests that the ten protons of the cation radical become equivalent by ring puckering. The complicated spectrum in fig. 1b is, therefore, associated with the cation radical prior to molecular motion.

Due to the poor resolution of fig. 1a it is not possible to obtain detailed information on the hyperfine structure for the cation radical of cyclopropane. However, a simulation assuming a set of six equivalent protons with a hfs constant of $\approx$5 G with a linewidth of 2 G for each component reproduced fairly well the observed spectrum in fig. 1a. As will be discussed later, the cation radical in the lowest-energy state is predicted to be distorted and its hfs constants are in-

equivalent. However, if the cation radical at 77 K undergoes a dynamic distortion just as the cation radical of cyclopentane at 100 K, the six protons will become equivalent on the time scale of the ESR hyperfine interaction. Such an averaging has been found for the cation radical of benzene in rigid matrices at 77 K [16,17].

4. Theoretical

Geometry optimization was performed by the energy gradient method with the HONDOG program [18, 19] where an unrestricted HF (UHF) wavefunction with the STO-4G minimal basis set [20] was employed.

The JT distortions are thought to be large for these σ-radicals and geometries were optimized for each of the irreducible spaces of lower symmetry [‡]. Hfs constants were calculated for the optimized geometries by applying the PO (pseudo-orbital) theory with a RHF wavefunction as reference wavefunction. We emphasize that we did not use the UHF wavefunction for the calculation of hfs constants. The UHF wavefunction does not satisfy spin-symmetry and its inadequacy for the calculation of spin correlation is well known [21]. On the other hand, the PO theory, which includes spin-polarized single excitations in a framework of the symmetry-adapted-cluster (SAC) expansion theory [22], satisfies pure spin-symmetry and takes a proper account of the spin correlation effect. It has been applied to various organic and inorganic radicals and fairly good results have been obtained [8—10]. Calculated hfs constants were analyzed by partitioning to spin-delocalization (SD) and spin-polarization (SP) contributions [23]. The SD contribution comes from the delocalization of the unpaired electron in the singly occupied orbital and is therefore always non-negative. On the other hand, the SP contribution comes from the spin correlation and becomes both positive and negative. The total hfs constant is the sum of these two contributions.

It is also important to select the basis set carefully

in the calculation of hfs constants because the basis set dependence of the calculated is not small. In a previous work [10], we used a double-ζ CGTO basis set which is contracted to be suited for the calculation of hfs constants [24] and obtained fairly good results. Here, the hfs constants of the cyclopropane cation radical were calculated with the double-ζ basis set and with the STO-4G minimal basis set at the geometry optimized with the latter basis set. In the appendix we show the difference in the calculated hfs constants: the difference is relatively small (3 G) for the proton but very large for carbon. For cyclopropane cations, the result of the double-ζ basis set is more reliable. For cyclobutane and cyclopentane cations, the hfs constants are calculated only with the STO-4G basis, and therefore the discussion is limited to the proton hfs constants.

5. Computational results and discussion

5.1. Cyclopropane

We first calculated the MOs of the neutral molecule for an experimentally determined D_{3h} geometry
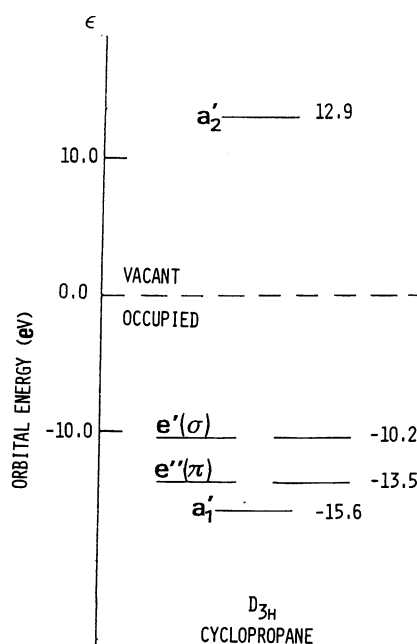

Fig. 2. Orbital energy levels of the neutral cyclopropane molecule.

[‡] In this study, the second derivatives of the energy along the pseudo-rotation valley were not calculated. Then, the "state" in the text means the point where the first derivatives of the energy surface become less than 10^{-3} au.

(r(CC) = 1.524 Å, r(CH) = 1.07 Å, ∠HCH = 120°) [25]
by a standard STO-4G basis. As shown in fig. 2, the
orbital symmetry of the HOMO is e′(σ) and the nature
of the orbital is in-plane σ bonding along the carbon
frame. The orbital next to the HOMO (NHOMO) has
e″(π) symmetry and its character is of σ bonding for
the C–H bonds and of π bonding for the C–C bonds
(cf. fig. 5). The σ bonding character is stronger than
the π one. According to the JT theory, the molecular
geometry will be distorted from D_{3h} to C_{2v} by remov-
ing an electron from one of these degenerate orbitals.

Fig. 3 shows the state correlation diagram. The JT
distortion associated with the e′(σ) orbital generates
$^2A_1$ and $^2B_2$ states of C_{2v} conformation. On the other
hand, the JT distortion associated with the NHOMO
e″(π) orbital yields $^2B_1$ and $^2A_2$ states. Thus, four
distinct electronic states are generated. Geometry op-
timization was performed for all of the four states of
C_{2v} symmetry. Fig. 4 shows the state level diagram
obtained for the fully optimized geometries.

The linear JT stabilization energy from the
$^2E′(D_{3h})$ state, was −36.7 and −33.2 kcal/mol for
$^2A_1$ and $^2B_2$, respectively obtained by open-shell RHF
with double-zeta basis set. The energy difference of
3.5 kcal/mol between $^2A_1$ and $^2B_2$ states given in fig.
4 corresponds to higher-order JT stabilization. Al-
though not shown in fig. 4 the first vertical excited
state of cyclopropane which has $^2B_2$ symmetry was as
high as 4.1 eV. This energy has been calculated by an
open-shell RHF wavefunction with a double-ζ basis
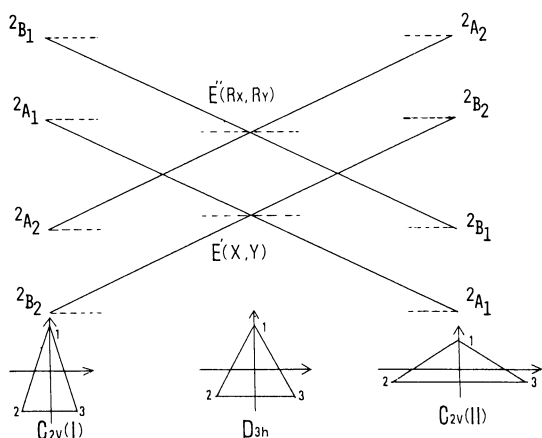set for the geometry optimized for the $^2A_1$ ground

state. The large excitation energy to this $^2B_2$ state
justifies the observed g = 2.0039 ± 0.0005, that is,
the possible anisotropy of the g-value originating from
the spin–orbit interaction is largely nullified by the
large energy separation between the ground $^2A_1$ and
the first vertical excited $^2B_2$ states.

Calculated geometries and hfs constants are shown
in figs. 5, 8 and 9 for cation radicals of cyclopropane,
cyclobutane, and cyclopentane, respectively. A com-
parison of the calculated proton hfs constants with
the experimental results is given in table 1. In the fol-
lowing, we explain the results of each radicals succes-
sively.

Fig. 5 shows the nodal pattern of the singly occu-
pied orbital, the geometry optimized with the STO-4G
basis, and the hfs constants calculated with the double-ζ
basis set (values in parentheses show SD and SP contri-
butions). Figs. 5a, 5b, 5c and 5d are for the $^2A_1$, $^2B_2$,
$^2B_1$ and $^2A_2$ states respectively.

The JT distortion in these doublet states can be un-
derstood with reference to the nodal pattern of the
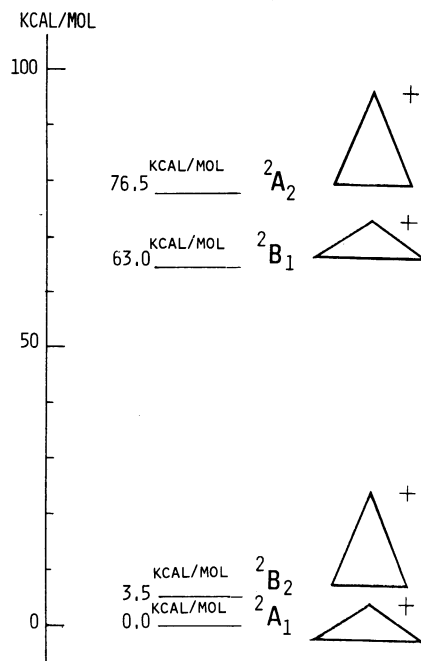singly occupied orbital; when an electron is removed

Fig. 4. State level diagram of the cation radical of cyclo-
propane. Result of the open-shell RHF wavefunction with the
double-ζ basis set.

Fig. 3. Correlation diagram of the cation radical of cyclo-
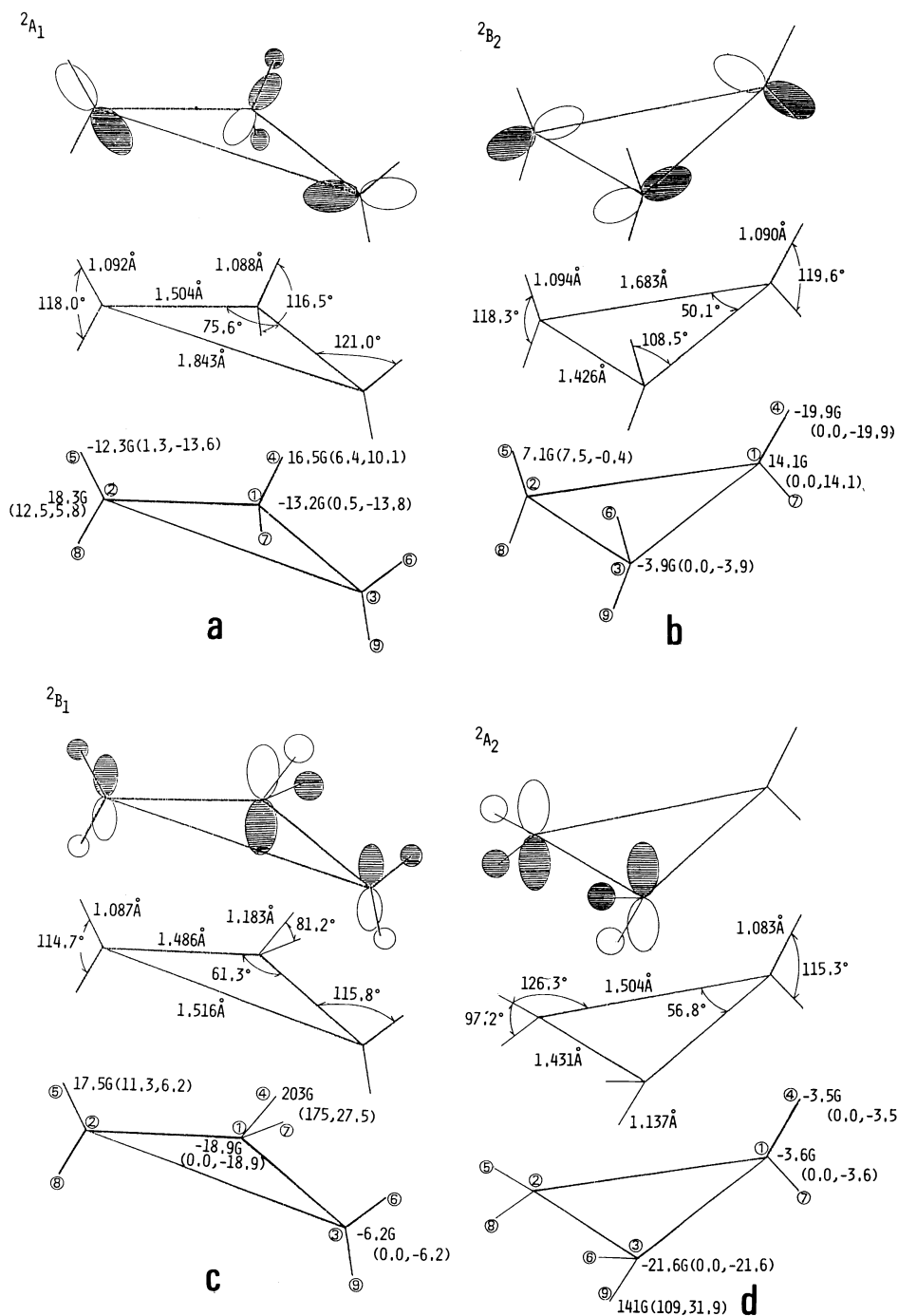propane.

Fig. 5. Nodal pattern of the singly occupied orbital in the optimized geometry and the hfs constants of the cyclopropane cation radical. Hfs constants are calculated by the PO theory with the double-ζ basis set. Experimental geometry of the neutral D_{3h} molecule is CC = 1.524 Å, CH = 1.07 Å, $\angle$HCH = 120°. SD and SP contributions of hfs constants are given in parentheses as (SD, SP) in gauss units.

Table 1
Proton hfs constants of cation radicals (in gauss)

Cation	State	Calc.	Exp.
cyclopropane (C$_{2v}$)	$^2A_1$	16.5	21 [a, b]
		−12.3	−12.5 [a, c]
			5.0 [d, f]
	$^2B_2$	−1.9 [d]	−
	$^2B_1$	79.3 [d]	−
	$^2A_2$	93.0 [d]	−
cyclobutane (D$_2$)	$^2B_3$	12.2 [d]	16.0 [e]
(C$_{2v}$)	$^2B_2$	18.5 [d]	−
cyclopentane (C$_s$)	$^2A''$	4.3 [d]	7.7

[a] Observed at 4 K by Triyama et al. [26].
[b] Two equivalent protons. See fig. 5a.
[c] Four equivalent protons. See fig. 5a.
[d] Averaged hfs constant.　　[e] Preliminary data.
[f] At 77 K.

from an orbital of antibonding nature, the bond will be shortened whereas the removal from a bonding orbital will cause bond elongation. In the $^2A_1$ state the stable geometry will be the flattened triangle II in fig. 3 because the singly occupied orbital of a_1 symmetry is antibonding between C_1 and C_2 and bonding between C_2 and C_3. In the $^2B_2$ state the singly occupied orbital is antibonding between C_2 and C_3 and bonding between C_1 and C_2 and between C_1 and C_3. The stable geometry will therefore be the vertically elongated triangle I in fig. 3. Similarly, the stable geometries for the $^2B_1$ and $^2A_2$ states originating from the $e''(R_x, R_y)$ orbitals are predicted as shown in fig. 3. In these states the change in the C–H length should be larger than that in the C–C length because the e'' orbitals are C–H σ bonding orbitals. The above qualitative predictions are, in fact, born out by the ab initio calculations as described below.

The two lowest states of the cyclopropane cation radical are calculated to be very close in energy as shown in fig. 4. The energy difference between the first two states $^2A_1$ and $^2B_2$ calculated by the open-shell RHF method with the double-ζ basis set (the UHF method with the STO-4G basis set) is only 3.5 (4.9) kcal/mol and that of the upper two states $^2B_1$ and $^2A_2$ is 13.5 (13.5) kcal/mol. The difference between the average of $^2A_1$ and $^2B_2$ and the average of $^2B_1$ and $^2A_2$ is 68.0 (82.8) kcal/mol. From the orbital energies shown in fig. 2 and the Koopmans theorem, the energy difference between the cationic states ob-

tainable from the vertical ionization from the $e'(\sigma)$ and $e''(\pi)$ orbitals is expected to be 3.3 eV (= 75.3 kcal/mol).

5.1.1. $^2A_1$ state

The nodal picture of the singly occupied orbital, the optimized geometry, and the hfs constants are shown in fig. 5a. The C_2–C_3 bond is elongated by as much as 0.32 Å and the C_1–C_2 and C_1–C_3 bonds are shortened by 0.02 Å relative to the neutral molecule. The HCH angles are 116.5° and 118.0° at C_1 and at C_2 and C_3 respectively (cf. ∠HCH = 120° in the neutral molecule). The total hfs constants are given with the components of SD and SP in parentheses. At the C_1 site, the carbon hfs constant is negative, −13.2 G, and the proton hfs is positive, 16.5 G, which is rather small in comparison with the experimental proton hfs value of 21 G observed at 4 K [26]. On the other hand, at the C_3 site, the carbon hfs value is positive, 18.3 G, and that of proton hfs is negative, −12.3 G. The calculated proton hfs constant agrees well with the experimental value of −12.5 G at 4 K [26]. The averaged hfs constants in this $^2A_1$ state are 7.8 and −2.7 G for carbon and proton, respectively.

5.1.2. $^2B_2$ state

The C_2–C_3 bond is shortened by 0.1 Å and the other two elongated by 0.16 Å as shown in fig. 5b. The change in the HCH angle is relatively small. The local electronic structure at C_1 is similar to that of the methyl radical and the proton hfs constant of −19.9 G comprises solely the SP contribution. The hfs constant of C_1 is also determined solely by the positive SP contribution, 14.1 G.

5.1.3. $^2B_1$ state

The relatively large change in the C_1–H_4 and C_1–H_7 bond lengths by 0.11 Å is reasonable because the singly occupied orbital has a σ bonding nature in the C–H bond region. The small HC_1H angle makes the overlap of the p-orbital of C_1 perpendicular to the molecular plane with the s-orbitals of H_4 and H_7 large. This leads to a SD contribution as large as 175 G and the total hfs constant amounts to 203 G at these protons. The experimental test of the predicted large hfs constant in this excited state may be interesting. For the carbon ring, the singly occupied orbital has a π nature and all of the carbon hfs constants comprised only the negative SP contributions.

5.1.4. $^2A_2$ state

The small HC_2H and HC_3H angles of $97.2°$ in fig. 5d are notable. As a result, a large hfs constant, 141 G, is predicted for the protons attached to C_2 and C_3. The largest carbon hfs value is -21.6 G at the bottom of the elongated triangle.

From the above result the ground state of the cation radical of cyclopropane is concluded to be the $^2A_1(\sigma)$ state. The proton hyperfine structure is characterized by the constants of -12.3 and 16.5 G (cf. fig. 5a) if the distortion is static. These theoretical results agree well with the experimental values, -12.5 and 21 G at 4 K. The observed spectrum, ≈ 5 G at 77 K is, however, much smaller. The apparent discrepancy may be removed if we consider that dynamic JT distortions within the $^2A_1$ state take place at 77 K. The averaged proton hfs value is -2.7 G in the $^2A_1$ state and it is comparable with the experimental value at 77 K.

In the above calculation, most of the discussion on the energies and hfs constants is based on the results of open-shell RHF and the PO theory with double-ζ CGTOs. The geometry optimization, however, was performed by the UHF wavefunction with the STO-4G basis set. The UHF wavefunction gives erroneous results when the spin contamination effect is large. To check the accuracy of our calculation, the degeneracy of the $^2E'(D_{3h})$ state was examined by the UHF wavefunction with the double-ζ CGTO. The calculated energy splitting was, however, only 0.89 kcal/mol. The s-square values were 0.773 and 0.756 for the doublet state. These small contaminations are due to the σ-radical nature of the cyclopropane cation. (In the case of the cyclopropenyl radical, which is a π-radical, the energy splitting by the UHF wavefunction is reported to be 14.8 kcal/mol and s-square is 1.12 for $^2E''(D_{3h})$ by Poppinger et al. [27].) The s-square values at optimized C_{2v} geometries were also checked by the STO-4G basis set. They were 0.790, 0.757, 0.759 and 0.762 for $^2A_1$, $^2B_2$, $^2B_1$ and $^2A_2$ respectively. Then the effect of spin contamination on the molecular geometry should be small for these σ-radicals.

5.2. Cyclobutane

Fig. 6 shows the orbital energy levels of the neutral cyclobutane molecule calculated for an experimentally determined geometry of D_{2d} symmetry ($r(CC) =$
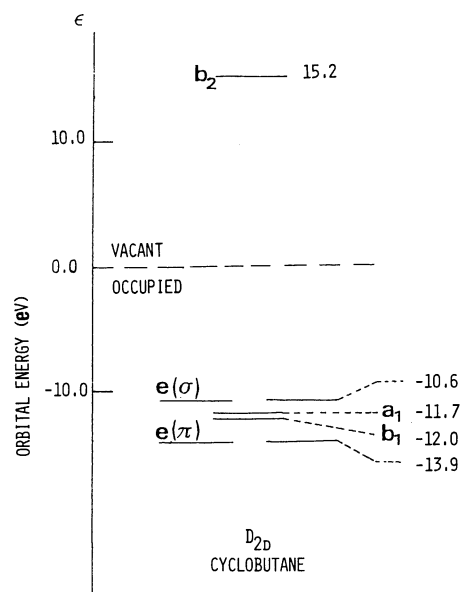

Fig. 6. Orbital energy levels of the neutral cyclobutane molecule.

1.555 Å, $r(CH) = 1.087$ Å, $\angle CCC = 87.2°$ and $\angle HCH = 108.6°$) [28]. HOMOs are degenerate with a σ nature in the carbon frame. Another set of e orbitals is at -13.9 eV. They are of a π nature in the carbon frame and of a σ nature in the CH bonds (cf. fig. 8). The cation radicals generated from these sets of e orbitals will be distorted from D_{2d} to C_{2v} or D_2 by the JT effect as shown in fig. 7. After geometry optimization, the most stable state is calculated to be $^2B_3$ of D_2 symmetry, and the next lowest state is $^2B_2$ of C_{2v} symmetry. However, these two states differ in energy only by 1.1 kcal/mol and therefore are almost degenerate.

In the normal mode connecting D_{2d} and D_2 geometries, the C_1-C_3 length is elongated and the C_1-C_2 length is shortened as shown in fig. 8. In D_2 symmetry, the cation of $^2B_3$ symmetry is more stable than the $^2B_2$ cation, since in the former the singly occupied orbital is bonding between C_1 and C_3 and antibonding between C_1 and C_2 as shown in the top of fig. 8a. In the normal mode connecting D_{2d} and C_{2v} geometries, the C_1-C_4 length is elongated and the C_2-C_3 length is shortened. Therefore, the $^2B_2$ state, in which the HOMO is bonding between C_1 and C_4 and antibonding between C_2 and C_3, is more stable than the counterpart $^2B_1$ state. Since the key interaction in the latter deformation is between non-bonding carbons, i.e.
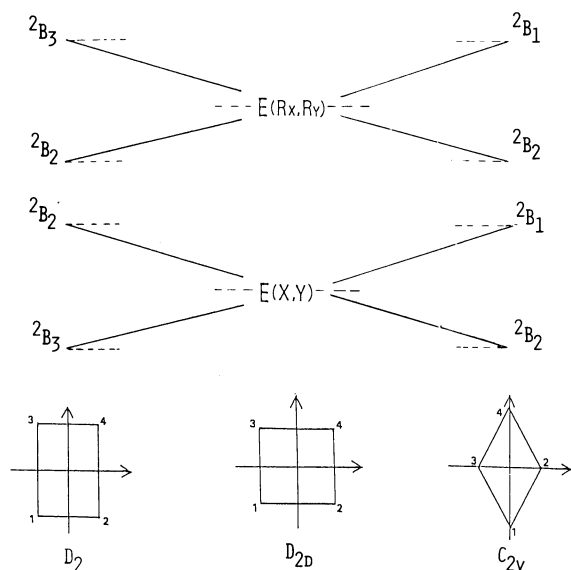
$^2B_3$ ____   ____ $^2B_1$

- - - E(Rx,Ry) - - -

$^2B_2$ ____   ____ $^2B_2$

$^2B_2$ ____   ____ $^2B_1$

- - - E(X,Y) - - -

$^2B_3$ ____   ____ $^2B_2$

D_2 D_{2D} C_{2v}

Fig. 7. Correlation diagram of the cation radical of cyclo-butane. The $^2B_3$ state of D_2 symmetry is calculated to be 1.1 kcal/mol more stable than the $^2B_2$ state of C_{2v} symmetry.

C_1–C_4 and C_2–C_3, the stabilization obtained by the Jahn—Teller distortion should be smaller than in the deformation from D_{2d} to D_2 geometry. The result of the ab initio calculation is parallel to this interpretation. The calculated energy difference is, however, as small as 1.1 kcal/mol. This is interpreted as due to a mixing between states of the same symmetry. In D_2 symmetry, the $^2B_3$ state originating from the E(R_x, R_y) state is higher in energy than the $^2B_2$ state, whereas in C_{2v} symmetry the $^2B_2$ state originating from the E(R_x,R_y) state is lower than the $^2B_1$ state (see fig. 7). Therefore, the stabilization of the ground state due to mixing with a higher state of the same symmetry is more advantageous for the C_{2v} distortion than for the D_2 distortion. Though this effect seems to be secondary, it works to diminish the energy difference between $^2B_3$ in D_2 and $^2B_2$ in C_{2v}.

5.2.1. $^2B_3$ state in D_2

The singly occupied orbital, the optimized geometry, and the hfs constants are given in fig. 8a. The
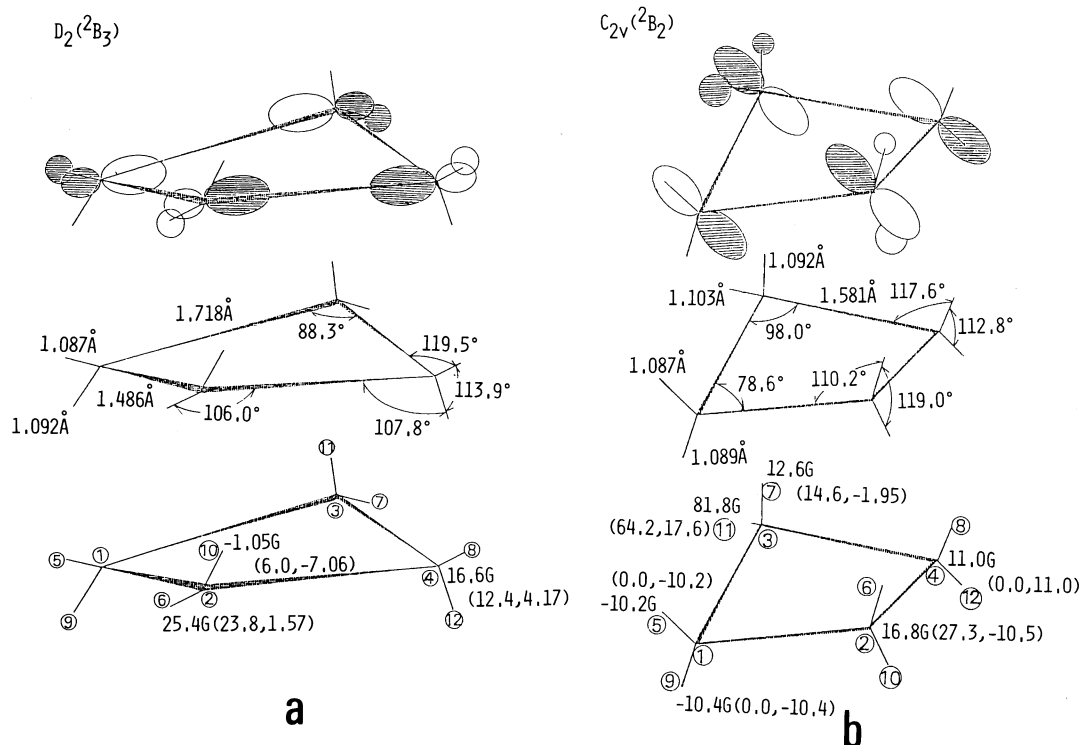

Fig. 8. Nodal pattern of the singly occupied orbital in the optimized geometry and the hfs constants of cyclobutane cation radical. Experimental geometry of the neutral D_{2d} molecule is CC = 1.555 A, CH = 1.087 A, ∠CCC = 87.2°, ∠HCH = 108.6°. SD and SP contributions of hfs constants are given in parentheses as (SD, SP) in gauss units.

bond between C_1 and C_3 is elongated by 0.16 Å and that of C_1 and C_2 is shortened by 0.07 Å relative to the neutral molecule. The hfs constant of the equatorial protons is calculated as 25.4 G which comprises the SD contribution of 23.8 G. This is due to a large overlap between the equatorial protons and the σ lobes of the singly occupied orbital as shown in fig. 8a.

5.2.2. $^2B_2$ state in C_{2v}

The distance between C_1 and C_4 is lengthened by by 0.24 Å and that of C_2 and C_3 shortened by 0.14 Å from 2.15 Å of the neutral D_{2d} geometry. These changes are very large partly because these pairs are non-bonding and are consistent with the nodal pattern of the singly occupied orbital. The hfs constant of the equatorial protons is as large as 81.8 G owing to a large overlap with the radical lobes.

The average proton hfs constant of the $^2B_3(D_2)$ state is 12.2 G and that of $^2B_2(C_{2v})$ is 18.5 G. As preliminary data, the experimental hfs constant is observed to be 16.0 as an averaged value of eight equivalent protons at 77 K and the theoretical hfs constant of the proton, 12.2 G in the $^2B_3(D_2)$ state, compares well with the experimental value.

5.3. Cyclopentane

The neutral molecule is known to undergo pseudo-rotation between C_s and C_2 conformations [7]. The cation radical is also considered to be distorted to C_s and C_2. In the present work ab initio calculations were made only for the C_s structure. The singly occupied orbital, the optimized geometry, and the hfs constants are given in fig. 9. In consistence with the singly occupied orbital, the C_1–C_2 and C_1–C_3 bonds are lenghtened by 0.14 Å from the neutral molecule [25]. The $C_2C_3C_4C_5$ frame is slightly distorted from D_{5h}. A large hfs constant of 43.4 G is calculated for the equatorial protons H_7 and H_8. The constants of H_6 and H_{11} are negative being contributed solely by SP. The average of the hfs constants becomes 4.3 G which is slightly smaller than the observed constant of 7.7 G in the spectrum of fig. 1c.

6. Conclusion

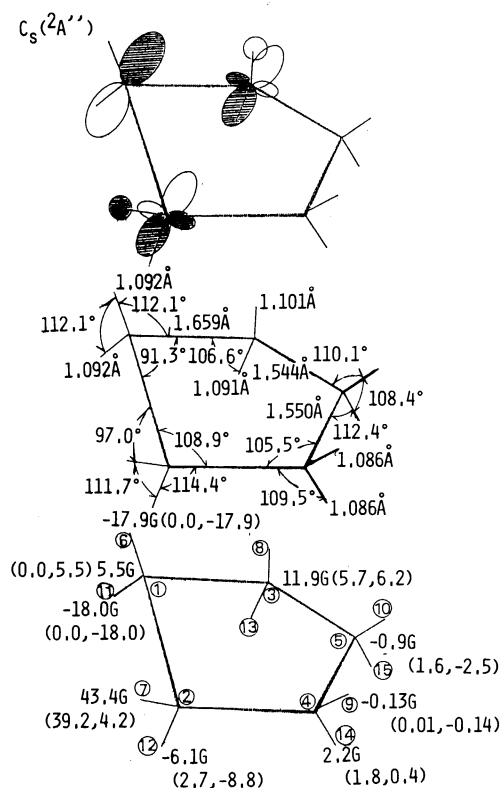In this work geometry optimization was carried

Fig. 9. Nodal pattern of the singly occupied orbital in the optimized geometry and the hfs constants of cyclopentane cation radical. Experimental geometry of the neutral D_{5h} molecule is CC = 1.52 Å, CH = 1.09 Å, $\angle$HCH = 109.5°. SD and SP contributions are given in parentheses as (SD, SP) in gauss units.

out for several electronic states of the cation radicals of three cycloalkanes. The calculated distortions relative to the neutral molecules are consistent with the nodal picture of singly occupied orbitals. Hfs constants calculated by the PO theory reflect the distortion of geometry sensitively through a large spin-delocalization. The calculated hfs constants agree well with the experimental results for the cation radicals of cyclopropane and cyclopentane if dynamic JT distortion is assumed.

Acknowledgement

work. They are also grateful to the Computer Center at the Institute for Molecular Science for the use of the Program Library HONDOG written by M. Dupuis, J. Rys and H.F. King, and for computer time. Part of this study was supported by a Grant-in-Aid for Scientific Research from the Japanese Ministry of Education, Science, and Culture.

Appendix

The hfs constants obtained by the double-ζ and STO-4G minimal basis sets are compared in table 2 for the $^2A_1$ ground state of the cyclopropane cation radical. The largest change in the calculated values is 21.2 G for the hfs constant of C_2 which is the bottom of the flattened triangle as shown in fig. 5a. Especially the SP contribution changed by as much as 31.1 G. The carbon hfs constant at the top of the triangle and the proton hfs constants have not changed so largely. In table 3 we show the differences in the averaged hfs constants for each of the four states of the cyclopropane cation. The carbon hfs constants in the $^2A_1$ and $^2B_2$ states have changed largely. The change in the proton hfs constant is $\approx 3-4$ G. For the upper two states, $^2B_1$ and $^2A_2$, the hfs constants increased for both the proton and carbon in the calculation with the STO-4G minimal basis set. In the $^2B_1$ state, the difference in the averaged proton hfs value

Table 2
Hfs constants of the cyclopropane cation radical in the $^2A_1$ state (in gauss) [a]

Nucleus [b]		Double ζ	STO-4G
C_1	SD	0.5	1.5
	SP	-13.8	-16.6
	total	-13.2	-15.1
C_2	SD	12.5	2.6
	SP	5.8	36.9
	total	18.3	39.5
H_4	SD	6.4	10.9
	SP	10.1	6.9
	total	16.5	17.9
H_5	SD	1.3	1.3
	SP	-13.6	-19.4
	total	-12.8	-18.1

[a] Result of the PO theory.
[b] See fig. 5a for the position of the nuclei.

Table 3
Averaged hfs constants of the cyclopropane cation (in gauss) [a]

State	Nucleus	Double ζ	STO-4G	Difference
$^2A_1$	C	7.8	21.3	13.5
	H	-2.7	-6.1	-3.4
$^2B_2$	C	2.1	18.9	16.8
	H	-1.9	-5.7	-3.8
$^2B_1$	C	-10.4	-4.3	6.1
	H	79.3	87.7	8.4
$^2A_2$	C	-15.6	-11.3	4.3
	H	93.0	96.3	3.3

[a] Result of the PO theory.

is rather large, i.e. 8.4 G. This comes from the large values at H_4 and H_7 in fig. 5c which are 203 and 230 G by the double-ζ and the STO-4G minimal basis sets, respectively.

References

[1] R. Englman, The Jahn–Teller effect in molecules and crystals (Wiley–Interscience, New York, 1972).
[2] E.R. Davidson and W.T. Borden, J. Chem. Phys. 67 (1977) 2191;
W.T. Borden, J. Am. Chem. Soc. 98 (1976) 2695;
E.R. Davidson and W.T. Borden, J. Am. Chem. Soc. 99 (1977) 2053;
D. Feller, W.T. Borden and E.R. Davidson, J. Chem. Phys. 74 (1981) 2256;
W.V. Volland, E.R. Davidson and W.T. Borden, J. Am. Chem. Soc. 101 (1979) 533;
W.T. Borden, E.R. Davidson and P. Hart, J. Am. Chem. Soc. 100 (1978) 388;
E.R. Davidson, W.T. Borden and J. Smith, J. Am. Chem. Soc. 100 (1978) 3299;
W.T. Borden and E.R. Davidson, J. Am. Chem. Soc. 101 (1979) 3771;
D. Feller, K. Tanaka, E.R. Davidson and W.T. Borden, J. Am. Chem. Soc. 104 (1982) 967.
[3] B. Sharf and J. Jortner, Chem. Phys. Letters 2 (1968) 68, and references therein.
[4] J.W. Rabalais, Principles of ultraviolet photoelectron spectroscopy (Wiley–Interscience, New York, 1977).
[5] H. Kubodera and T. Shida, 23rd Symposium on Radiation Chemistry, Kyoto, October 1980.
[6] M. Iwasaki, K. Toriyama and K. Nunome, J. Am. Chem. Soc. 103 (1981) 3591.
[7] D. Cremer and J.A. Pople, J. Am. Chem. Soc. 97 (1975) 1358;
E. Diez, A.L. Esteban, F.J. Bermejo and M. Rico, J. Phys. Chem. 84 (1980) 3191.

[8] H. Nakatsuji and K. Hirao, Chem. Phys. Letters 47 (1977) 569.

[9] H. Nakatsuji and K. Hirao, J. Chem. Phys. 68 (1978) 4279.

[10] K. Ohta, H. Nakatsuji, K. Hirao and T. Yonezawa, J. Chem. Phys. 73 (1980) 1770.

[11] T. Shida and T. Kato, Chem. Phys. Letters 68 (1979) 106;
T. Shida, Y. Egawa and H. Kubodera, J. Chem. Phys. 73 (1980) 5963;
T. Shida, H. Kubodera and Y. Egawa, Chem. Phys. Letters 79 (1981) 179;
H. Kubodera, T. Shida and K. Shimokoshi, J. Phys. Chem. 85 (1981) 2583.

[12] K. Toriyama, K. Nunome and M. Iwasaki, J. Chem. Phys. 85 (1981) 2149.

[13] M.C.R. Symons and I.G. Smith, J. Chem. Res. S (1979) 382.

[14] J.T. Wang and F. Williams, J. Phys. Chem. 84 (1980) 3156.

[15] B.G. Segal, M. Kaplan and G.K. Fraenkel, J. Chem. Phys. 43 (1965) 4191.

[16] M.K. Carter and G. Vincow, J. Chem. Phys. 47 (1967) 292.

[17] O. Edlund, P.-O. Kinell, A. Lund and A. Shimizu, J. Chem. Phys. 46 (1967) 3679.

[18] H.F. King, M. Dupuis and J. Rys, Program Library, HONDOG, Program No. 343, Computer Center, Institute for Molecular Science, Okazaki (1979).

[19] M. Dupuis, J. Rys and H.F. King, Quantum Chemistry Program Exchange, Program No. 338, Chemistry Department, Indiana University, Bloomington (1977);
J. Chem. Phys. 65 (1976) 111;
M. Dupuis and H.F. King, J. Chem. Phys. 68 (1978) 3998.

[20] W.J. Hehre, R.F. Stewart and J.A. Pople, J. Chem. Phys. 51 (1969) 2657.

[21] H. Nakatsuji, J. Chem. Phys. 59 (1973) 2586.

[22] H. Nakatsuji and K. Hirao, J. Chem. Phys. 68 (1978) 2053.

[23] H. Nakatsuji, H. Kato and T. Yonezawa, J. Chem. Phys. 51 (1969) 3175.

[24] Y. Ellinger, A. Rassat, R. Subra and G. Berthier, J. Chem. Phys. 61 (1975) 1.

[25] Landolt–Börnstein, Structural data of free polyatomic molecules, New Series, Vol. II/7, eds. K.-H. Hellwege and A.M. Hellwege (Springer, Berlin, 1976).

[26] K. Triyama, K. Nunome and M. Iwasaki, 21th ESR symposium, Tsukuba, Japan (1982).

[27] D. Poppinger, L. Radom and M.A. Vincent, Chem. Phys. 23 (1977) 437.

[28] L.E. Sutton, ed., Tables of interatomic distances and configuration in molecules and ions (The Chemical Society, London, 1958, 1965).